



III

Publication III

M.O.K. Särkelä, M.J. Ermes, M.J. van Gils, A.M. Yli-Hankala, V.H. Jäntti, A.P. Vakkuri. 2007. Quantification of epileptiform electroencephalographic activity during sevoflurane mask induction. *Anesthesiology* 107, no. 6, pages 928-938.

© 2007 The American Society of Anesthesiologists, Inc. Lippincott Williams & Wilkins, Inc.

Reprinted with permission.

Quantification of Epileptiform Electroencephalographic Activity during Sevoflurane Mask Induction

Mika O. K. Särkelä, M.Sc.,* Miiikka J. Ermes, M.Sc.,† Mark J. van Gils, Ph.D.,‡ Arvi M. Yli-Hankala, M.D., Ph.D.,§ Ville H. Jäntti, M.D., Ph.D.,|| Anne P. Vakkuri, M.D., Ph.D.#

Background: Sevoflurane may induce epileptiform electroencephalographic activity leading to unstable Bispectral Index numbers, underestimating the hypnotic depth of anesthesia. The authors developed a method for the quantification of epileptiform electroencephalographic activity during sevoflurane anesthesia.

Methods: Electroencephalographic data from 60 patients under sevoflurane mask induction were used in the analysis. Electroencephalographic data were visually classified. A novel electroencephalogram-derived quantity, wavelet subband entropy (WSE), was developed. WSE variables were calculated from different frequency bands. Performance of the WSE in detection and quantification of epileptiform electroencephalographic activity and the ability of the WSE to recognize misleading Bispectral Index readings caused by epileptiform activity were evaluated.

Results: Two WSE variables were found to be sufficient for the quantification of epileptiform activity: WSE from the frequency bands 4–16 and 16–32 Hz. The lower frequency band was used for monophasic pattern monitoring, and the higher frequency band was used for spike activity monitoring. WSE values of the lower and higher bands followed the time evolution of epileptiform activity with prediction probabilities of 0.809 (SE, 0.007) and 0.804 (SE, 0.007), respectively. In deep anesthesia with epileptiform activity, WSE detected electroencephalographic patterns causing Bispectral Index readings greater than 60, with event sensitivity of 97.1%.

Conclusions: The developed method proved useful in detection and quantification of epileptiform electroencephalographic activity during sevoflurane anesthesia. In the future, it may improve the understanding of electroencephalogram-derived information by assisting in recognizing misleading readings of depth-of-anesthesia monitors. The method also may assist in minimizing the occurrence of epileptiform activity and seizures during sevoflurane anesthesia.

SEVOFLURANE is a nonpungent, short-acting volatile anesthetic agent. Clinical trials have confirmed its suitability for mask induction in children¹ and in adults.²

* Research Scientist, GE Healthcare Finland Oy. † Research Scientist, ‡ Senior Research Scientist, VTT Technical Research Centre of Finland. § Research Professor, Department of Anesthesia, Tampere University Hospital and University of Tampere. || Department of Clinical Neurophysiology, Tampere University Hospital. # Head of the Department of Anesthesia, Peijas Hospital, Helsinki University Hospital.

Received from GE Healthcare Finland Oy, Helsinki, Finland; VTT Technical Research Centre of Finland, Tampere, Finland; Helsinki University Hospital, Helsinki, Finland; Tampere University Hospital, Tampere, Finland; and University of Tampere, Tampere, Finland. Submitted for publication February 6, 2007. Accepted for publication August 15, 2007. Supported by Helsinki University Central Hospital Research Fund No. TYH9242 from Helsinki University Hospital, Helsinki, Finland, and by Tekes (the Finnish Funding Agency for Technology and Innovation), Helsinki, Finland. M. Särkelä is an employee GE Healthcare Finland Oy, Helsinki, Finland. Drs. Yli-Hankala and Vakkuri are medical advisors of GE Healthcare Finland Oy.

Address correspondence to M. Särkelä: GE Healthcare Finland Oy, P.O. Box 900, 00031 GE, Finland. mika.sarkela@ge.com. Information on purchasing reprints may be found at www.anesthesiology.org or on the masthead page at the beginning of this issue. ANESTHESIOLOGY's articles are made freely accessible to all readers, for personal use only, 6 months from the cover date of the issue.

Many studies have documented that sevoflurane may induce epileptiform electroencephalographic activity,^{3–8} and seizure-like movements have been described.⁹ Despite these observations, sevoflurane remains one of the most widely used volatile anesthetics.

In current anesthesia practice, electroencephalogram and electroencephalogram-derived variables, such as the Bispectral Index (BIS; Aspect Medical Systems, Norwood, MA) are often used to monitor the hypnotic component of anesthesia. BIS is composed of the weighted sum of three features derived from spectral, bispectral, and time-domain contents of the electroencephalogram.¹⁰ BIS has been shown to decrease consistently with increasing sevoflurane end-tidal concentrations and decreasing Observer's Assessment of Alertness and Sedation scale score,¹¹ as well as with increasing estimated sevoflurane effect site concentrations.^{12,13} However, during stable and deep sevoflurane anesthesia, BIS has been reported to increase during epileptiform activity⁵ or to fluctuate abnormally.¹⁴

The objective of this study was to develop a method for the automatic detection and quantification of epileptiform electroencephalographic waveforms during sevoflurane anesthesia to improve the reliability of electroencephalographic monitoring.

Materials and Methods

Electroencephalographic Data

Electroencephalographic data from two previously published studies were used.^{4,6} Both studies had institutional approval (Ethics Committee of the Department of Obstetrics and Gynecology, Helsinki University Hospital, Helsinki, Finland), and each patient gave written informed consent. Data were obtained from 60 patients with American Society of Anesthesiologists physical status I or II, scheduled to undergo elective gynecological surgery. Exclusion criteria were age older than 50 or younger than 18 yr; history of cardiac, pulmonary, or neurologic disease; body mass index greater than 28 kg/m²; history of esophageal reflux; or alcohol or drug abuse.

All patients breathed oxygen *via* a clear facemask for 2 min before anesthetic induction. Anesthesia was induced with a single-breath method *via* a facemask using sevoflurane (8% in nitrous oxide, 50% in oxygen) with a semiclosed anesthesia system containing a carbon dioxide absorber and primed with a fresh gas flow of 10 l/min. Nitrous oxide was used according to our routine clinical practice. The patients were asked to exhale

forcefully to the residual volume, followed by a vital capacity breath with a facemask placed tightly over the nose and the mouth; they were then asked to hold their breath as long as possible. Thereafter, the patients were allowed to breathe normally until loss of consciousness (LOC). After LOC, anesthetic induction continued *via* four different techniques: (1) spontaneous breathing for 6 min after the first breath from the facemask, (2) controlled hyperventilation for 6 min after the first breath, (3) spontaneous breathing for 2 min after LOC followed by controlled hyperventilation for 3 min, and (4) controlled hyperventilation for 5 min after LOC. Anesthesia techniques 1 and 2 were used in the work of Yli-Hankala *et al.*,⁴ and techniques 3 and 4 were used in the work of Vakkuri *et al.*,⁶ wherein the anesthetic methods are described in more detail. Because of technical difficulties, synchrony between the time stamps of the first breaths and the electroencephalographic data were absent for six patients with anesthesia techniques 1 and 2.

Electroencephalographic measurements were performed with Zipprep electrodes (Aspect Medical Systems) positioned on both temporal bones laterally to the eyes; both mastoid bones; Fp1; Fp2; Fpz; and the ground electrode at the center of the forehead, between the eyebrows. A four-channel electroencephalogram was recorded with an Aspect A-1000[®] monitor (Aspect Medical Systems) using the following electrode pairs: Fp1 and left mastoid, Fp2 and right mastoid, Fpz and left temporal, and Fpz and right temporal. Impedances below 5 kΩ were considered acceptable. The electroencephalogram was collected at a sample frequency of 128 Hz; spectral analysis revealed that the collected electroencephalogram contained frequencies up to 47 Hz. Processed variables of the A-1000[®] monitor were collected at 5-s intervals, including BIS (version 3.0), burst suppression ratio (BSR), and signal quality index (SQI) from all four channels. Data recording was performed with a laptop computer using Datalogger software (Aspect Medical Systems).

Electroencephalographic analyses were conducted by a neurophysiologist familiar with the anesthesia electroencephalogram (V.J.). The electroencephalographic phenomena were classified as δ activity (<4 Hz; D), slow δ activity (<2 Hz; DS), slow δ monophasic activity (DSM), slow δ monophasic activity with spikes (DSMS), burst suppression (BS), burst suppression with spikes (SBS), polyspikes, rhythmic polyspikes, and periodic epileptiform discharges. Polyspikes refers to a waveform with more than two negative and positive deflections; rhythmic polyspikes to polyspikes appearing at regular intervals; and periodic epileptiform discharges to bilateral, periodic complexes. To simplify algorithm development, the three latter classes were combined into one class, labeled periodic discharges (PD), mainly because the exact definition of time instants for transitions between these classes is problematic even for an experi-

enced neurophysiologist. Electroencephalographic data before the onset of δ activity were classified as awake (AW). The electroencephalographic data periods including D or DS classes were considered to be associated with nonepileptiform activity. Although slow monophasic pattern is not typically considered as epileptiform,⁸ monophasic pattern preceded spike activity and spikes seemed to emerge as superimposed onto the monophasic pattern (fig. 1). Therefore, monophasic pattern may have an important role in monitoring as a predictive indicator of spike activity. The periods including DSM,

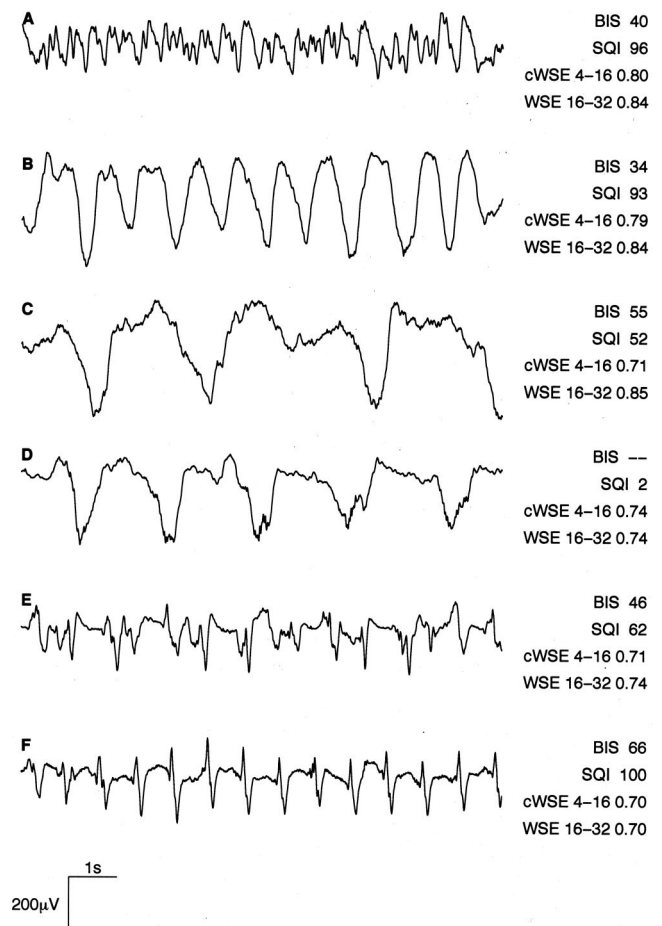


Fig. 1. Classified electroencephalogram phenomena and the corresponding Bispectral Index (BIS), signal quality index (SQI), combined wavelet subband entropy (cWSE) 4–16 Hz, and wavelet subband entropy (WSE) 16–32 Hz values. (A) δ activity, (B) slow δ activity, (C) slow δ monophasic activity, (D) slow δ monophasic activity with spikes, (E) polyspikes, and (F) rhythmic polyspikes. E and F were placed in the same periodic discharges class. Typically, BIS decreased constantly during deepening anesthesia until slow δ activity gave way to slow δ monophasic activity. Here, BIS is not displayed during slow δ monophasic activity with spikes (D). The simultaneous SQI reading is 2, suggesting a high number of false positives in the artifact detection algorithm. Periodic discharges tended to increase BIS values. Here, during rhythmic polyspikes (F) occurring during deep level of hypnosis, the SQI is 100, suggesting a reliable BIS estimate. cWSE 4–16 Hz values decreased when a monophasic pattern appeared in the electroencephalogram. WSE 16–32 Hz values decreased with increasing spike amplitudes.

Table 1. Overview of Electroencephalographic Class Distributions in the Development, Test, and Full Data Sets

Class	Development Data		Test Data		All Data	
	Incidence out of 30	Duration, h:mm:ss	Incidence out of 30	Duration, h:mm:ss	Incidence out of 60	Duration, h:mm:ss
AW	30	0:54:21	30	0:57:33	60	1:51:54
D	28	0:26:41	28	0:24:27	56	0:51:58
DS	22	0:20:49	22	0:24:08	44	0:44:57
DSM	26	0:28:40	28	0:27:11	54	0:55:51
DSMS	14	0:15:20	14	0:18:54	28	0:34:14
PD	22	1:27:00	25	1:33:58	47	3:00:58
BS	8	0:22:00	4	0:14:38	12	0:36:38
SBS	4	0:08:50	3	0:06:10	7	0:15:00

AW = awake activity; BS = burst suppression; D = δ activity; DS = slow δ activity; DSM = slow δ monophasic activity; DSMS = slow δ monophasic activity with spikes; PD = periodic discharges; SBS = burst suppression with spikes.

DSMS, or PD were therefore considered to be associated with epileptiform activity in this study. Table 1 (“All data” column) presents the distribution of the data over the different electroencephalographic classes. Figure 1 illustrates some examples of the different electroencephalographic classes. Movements of eyes and head during the awake state caused artifacts. In this phase of our study, we focused on the electroencephalogram during anesthesia, and therefore, these artifacts were not removed.

Feature Generation

We present a novel quantity, wavelet subband entropy (WSE), for characterizing the evolution of the epileptiform electroencephalogram waveforms. WSE is based on a dyadic multiresolution decomposition of the signal performed with a discrete wavelet transform using the Mallat algorithm.¹⁵

A wavelet is an oscillating function whose energy is concentrated in time to better represent transient, non-stationary signals. For a function to qualify as a wavelet, it must exhibit certain mathematical properties, one of which is to have band-pass filter characteristics. In the wavelet transform, correlation between the signal under observation and the used wavelet basis function is derived, similarly to the Fourier transform. According to its mathematical definition, the Fourier transform uses infinitely continuing sine and cosine functions as basis functions. In the wavelet transform basis functions are selected beforehand from the classes of mother wavelets. The wavelet basis functions are created from the mother wavelet by scaling and translating it in time. As a result, the wavelet transform produces information of both scale and time of each signal component, whereas the Fourier transform gives information only about the frequency contents of the signal. The fundamental idea of analyzing a signal at different scales is called multiresolution analysis. Because of their better time-localization property and the possibility to select differently shaped basis functions, wavelets can be more effective than the Fourier transform in describing steeply varying or distinctly localized signals, such as spikes and bursts.¹⁶

The Mallat algorithm computes the discrete wavelet transform using a cascade implementation of filter banks of two quadrature mirror filters. At each level of signal decomposition, two filters are used, a low-pass filter and a high-pass filter, both followed by down-sampling the filter output by two. The obtained down-sampled output samples are wavelet coefficients (c_j) at a certain scale j . Output samples from the low-pass filtering are approximation coefficients (a_j), characterizing original signal on a coarse degree, whereas samples obtained from the high-pass filtering are detail coefficients (d_j), characterizing the signal on a fine degree. Detail coefficients d_j , at each scale j and translation index k , are correlations between the observed signal $x(t)$ and the discretized mother wavelet $\psi_{j,k}(t)$:

$$d_j(k) = \int_{-\infty}^{\infty} x(t) \psi_{j,k}(t) dt \quad (1)$$

Similarly, approximation coefficients are correlations between the observed signal and the discretized scaling function, which is orthonormal to the mother wavelet. When the mother wavelet and scaling function are discretized in a dyadic manner, *i.e.*, scale and translation are discretized with steps of 2^j , the original signal can still be reconstructed from the obtained detail and approximation coefficients.¹⁵ After each level of signal decomposition, approximation coefficients are supplied to an identical filter bank operation, thus leading to a finer representation of the signal at scale $j + 1$. The obtained approximation and detail coefficients create a dyadic multiresolution representation of the original signal. As can be inferred from equation 1, it is advantageous to use mother wavelets that are intrinsically well adapted to represent the original signal. This leads to better time localization of the desired signal waveforms, *i.e.*, fewer coefficients required to accurately describe the original signal.¹⁷

We performed the Mallat algorithm with three different mother wavelets (fig. 2): Daubechies 1, Daubechies

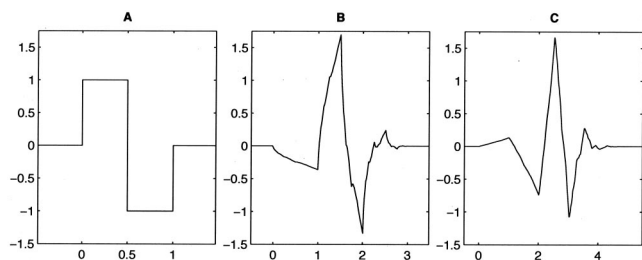


Fig. 2. The mother wavelets used in the study: (A) Daubechies 1, (B) Daubechies 2, and (C) Daubechies 3.

2, and Daubechies 3.¹⁸ The Daubechies wavelet family was selected because Daubechies 1 is a unique mother wavelet composed of square waves, thus being potentially suitable to capture characteristics of monophasic patterns. Higher-order mother wavelets Daubechies 2 and Daubechies 3 are more spiky, therefore potentially being better able to capture spiky electroencephalographic waveforms. Daubechies wavelets of the order four and higher also exist, but they are more expanded in time axis and more sinusoidal-like. Therefore, they are probably less suitable for our purposes to capture transient and spiky waveforms. Other wavelet families, such as Coiflets and Symlets, also include spiky mother wavelets. The Mallat algorithm was performed like a conventional signal filtering, starting from the first recorded sample and ending with the last sample of the data record. After processing the signal with the Mallat algorithm, wavelet coefficients were obtained at five scales: $d_1, a_1, d_2, a_2, d_3, a_3, d_4, a_4, d_5,$ and a_5 , which roughly correspond to frequency bands 32–64, 0–32, 16–32, 0–16, 8–16, 0–8, 4–8, 0–4, 2–4, and 0–2 Hz, respectively. Wavelet analysis was conducted with Matlab Wavelet Toolbox (version 2.2; The MathWorks Inc., Natick, MA), whose user’s guide^{19**} is recommended reading as an introduction to wavelet analysis.

Wavelet coefficients c_j (both approximations $[a_j]$ and details $[d_j]$) at each scale j , with each mother wavelet and within each 5-s epoch, sliding at 1-s intervals, were squared and normalized according to the equation:

$$\hat{c}_j(n) = \frac{c_j(n)^2}{\sum_{m=1}^{N_j} c_j(m)^2}, \tag{2}$$

where c_j are coefficients at a certain scale j , N_j is the number of coefficients at each scale j within a given epoch, n is the index used within each 5-s epoch, and m is the summation index. The coefficients \hat{c}_j at each scale were analyzed with the relative form of the Shannon

entropy equation²⁰; the resulting value is called wavelet subband entropy (WSE):

$$WSE_{\hat{c}_j} = - \frac{\sum_{n=1}^{N_j} \hat{c}_j(n) \cdot \log \hat{c}_j(n)}{\log N_j}. \tag{3}$$

Squaring (equation 2) makes coefficients nonnegative, which is a necessity for the application of the entropy equation. Furthermore, it enhances the contribution of high-amplitude signal values in relation to lower-amplitude signal values, making the entropy equation more sensitive to the characteristic features of epileptiform activity. Normalization (equation 2) makes WSE insensitive to changes in the total signal power. Equation 3 can be interpreted as a “distance” between the wavelet basis function and the original signal.¹⁷

Feature Selection

Epileptiform activity in the data were characterized mainly by two morphologically different waveforms: monophasic waves resembling K complexes of natural sleep and spikes. Our goal was to find optimal features for the monitoring of these two waveforms. The second goal was to develop a user-friendly method that works with a minimal set of electrodes. Therefore, our aim was to use only one-channel data for the final analysis.

Data were randomly divided into two sets, development and test data (table 1), so that both of the sets contained approximately the same number of cases representing each of the four anesthesia techniques. The development data set was used for feature selection and method development. The test data set was used for performance assessment.

Epileptiform activity evolved typically from D to DS and then to DSM, DSMS, and PD, in that sequence. A monophasic pattern appeared at the transition from DS to DSM. The optimal feature set for detecting presence of monophasic patterns was selected on the basis of the performance of a linear discriminant classifier developed to discriminate between two groups of electroencephalographic classes. Groups were a union of D and DS classes and a union of DSM, DSMS, and PD classes. The root-mean-square error was used as performance criterion of the classifier. The total group of potentially useful features contained 120 features; WSE values from the aforementioned 10 bands with 3 different mother wavelets at 4 channels, creating $10 \times 3 \times 4 = 120$ features. The optimal feature set was found using a feature selection algorithm, sequential floating forward search,²¹ effectively implementing an iterative stepwise regression algorithm but allowing for backtracking (possible removal of earlier selected features). Backtracking alleviates the potential problem of so-called nesting, the situation when, once a feature has been added to a feature subset, it cannot be removed anymore in later iterations.

** Available at: <http://www.mathworks.com/access/helpdesk/help/toolbox/wavelet/>. Accessed August 16, 2007.

Table 2. Division into Different Electroencephalographic Classes for Classifier Development and Performance Evaluation

Class	Monophasic Pattern Present	Spike Present	Severity
AW	Not used	Not used	Not used
D	No	No	0
DS	No	No	0
DSM	Yes	No	1
DSMS	Yes	Yes	2
PD	Yes	Yes	3
BS	Not used	Not used	Not used
SBS	Not used	Not used	Not used

AW = awake activity; BS = burst suppression; D = δ activity; DS = slow δ activity; DSM = slow δ monophasic activity; DSMS = slow δ monophasic activity with spikes; PD = periodic discharges; SBS = burst suppression with spikes.

Nesting may lead to suboptimal feature set selections. Considering the limited number of cases and for practical monitoring reasons, the size of optimal feature set was predefined to be maximally three. If the increase in performance by adding a next best feature was minimal (below a preset threshold), the feature selection process was stopped even if the number of three features was not reached, thus potentially leading to feature set sizes of smaller than three. To enable the use of one-channel electroencephalographic monitoring different classifiers and thus different optimal feature sets, were developed for the four different channels separately (*i.e.*, using only features from one single channel). The channel with the best-performing feature set was then chosen for the implementation. Similarly, the optimal feature set for spike activity monitoring was obtained using sequential floating forward search with a linear discriminant classifier that aimed to discriminate between the D, DS, and DSM groups and the DSMS and PD groups. Table 2 illustrates the division and labeling of the classes.

Performances of different best-performing classifiers were initially assessed with receiver operating characteristic (ROC) curve analysis. An ROC plot displays the sensitivity of the detector *versus* (1 – specificity) for all possible cutoff values.¹⁶ For the detection of monophasic patterns, we conducted additional ROC curve analysis where only DS and DSM classes were included. This was done to emphasize the method's ability for detecting the important stage when a monophasic pattern starts to emerge, thus being the first predictive indicator of the upcoming spike activity.

Cutoff values for monophasic pattern and spike detection were specified using the ROC plot analysis. To select the optimal cutoff point, we need to evaluate the effects of false-positive and false-negative results. Here, both of these effects were considered equal, and the optimal cutoff value was found by looking for the point on the curve with the smallest distance to sensitivity = 1 and specificity = 1.¹⁶

Performance Evaluation

The optimal feature sets' performances were assessed using prediction probability, sensitivity, and specificity analyses using the test data set. Prediction probability (P_K) is commonly used to study the performance of anesthetic depth indicators,²² where it quantifies the concurrence between the correct behavior of the anesthetic depth indicator with the observed depth of anesthesia. We calculated P_K values for each optimal feature set's ability to predict the class of electroencephalographic waveforms described. The electroencephalographic classes were labeled according to increasing severity of the epileptiform activity (arguments for this: see Discussion). In our classification, D and DS presented waveforms without epileptiform activity and were labeled 0, DSM presented mild severity and was labeled 1, DSMS presented moderate severity and was labeled 2, and PD presented a severe pattern and was labeled 3. In addition, we calculated P_K values for the monophasic pattern detection and the spike activity detection. To compensate for bias and allowing derivation of robust estimates of SEs and confidence intervals (CIs), P_K values were estimated using the jackknife method. In this case, for a sample of n data points, the method requires computation of $n + 1$ estimates of P_K ; one from the total sample of n points and n estimates calculated from subsets obtained by deleting one different data point per estimation. Cutoff values obtained from the development data set were used to calculate sensitivity and specificity over the test data set. Table 2 illustrates the division and labeling of the electroencephalographic classes used to evaluate the method's ability to detect monophasic patterns and spikes, and P_K analysis for evolutionary electroencephalogram waveforms.

BIS and WSE during Epileptiform Activity

To study the behavior of BIS, the SQI, and the WSE variables of the optimal feature sets during epileptiform activity, mean, SD, median, and quartiles for each variable were calculated for each electroencephalographic class. Normality of the distribution of the variables was assessed with the Kolmogorov-Smirnov test. In case the variable distribution was found to be significantly different from the normal distribution, a nonparametric pairwise test was used to assess differences between feature values of evolutionarily successive electroencephalographic classes. More specifically, for each patient, average feature values for each class were calculated and compared with the Wilcoxon signed rank test (SPSS version 14.0; SPSS Inc., Chicago, IL). A value of $P < 0.05$ was considered significant in all tests. In some instances, the BIS algorithm was incapable of calculating reliable BIS values; in those cases, the value was not displayed on the monitor screen. We analyzed BIS-not-displayed time as a proportion of total time in each electroencephalographic class.

We examined BIS and WSE values at a deep level of hypnosis, using 2 min 30 s as the period of focus, starting 3 min after the first breath of the inhalation induction. LOC was registered for 30 patients with anesthesia techniques 3 and 4. The median time from the beginning of mask induction to LOC was 45 s, and the range was 30–100 s. In 54 patients, the median time delay from the first facemask breath to the appearance of δ or slow δ activity was 63 s, with a range of 34–171 s. End-tidal sevoflurane concentrations for patients with anesthesia techniques 1 and 2 were 4.4–6.5% during the time period studied.

We estimated the capability of our method to detect the situation where BIS was greater than 60 despite a deep level of hypnosis during the inspection time. Detection was defined to have occurred if either of the WSE variables was equal to or below its cutoff value. Event sensitivity was calculated with the any-overlap method. The any-overlap is the traditional method used in studying the accuracy of automatic seizure detectors.²³ The method calculates the ratio of matched seizures (an algorithm seizure overlaps a seizure as annotated by a human expert) by the total number of expert-annotated seizures in the record. Our method’s event sensitivity was calculated as the ratio of detections over the total number of events when BIS was constantly greater than 60. In addition, we conducted a pairwise comparison between BIS and WSE variables by calculating traditional sensitivity as a ratio of detections and the total number of BIS readings greater than 60. All analyses were performed with Matlab 6.5 and 7.1 (The MathWorks, Inc.).

Results

Feature Selection

Channel Fp2–right mastoid proved to be the best channel in terms of performance with a linear discriminant classifier. Channel Fp1–left mastoid was almost equally good, whereas the other two channels were considerably worse in their performance. The WSE of coefficients (using mother wavelet Daubechies 1) corresponding to frequency bands 4–8 and 8–16 Hz obtained the best classification performance for monophasic pattern detection. The WSE variable for the detection of monophasic patterns was a combination of WSE (cWSE) from the two frequency bands:

$$cWSE_{4-16\text{ Hz}} = 0.4391 \cdot WSE_{4-8\text{ Hz}} + 0.5609 \cdot WSE_{8-16\text{ Hz}} \quad (4)$$

Weights for equation 4 were obtained from the linear regression analysis. On the basis of ROC curve analysis, detection of monophasic patterns was set to occur when cWSE 4–16 Hz was equal or below the cutoff value 0.78. The ROC curve for monophasic pattern detection is illustrated in figure 3.

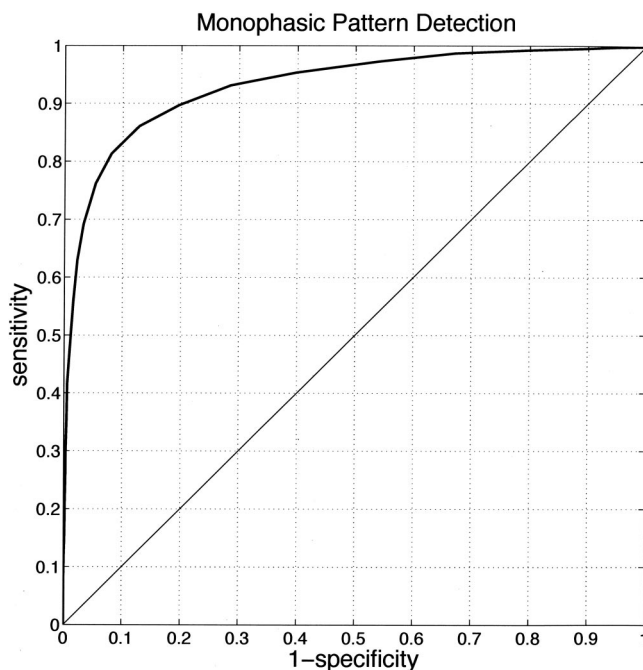


Fig. 3. The receiver operating characteristic curve for monophasic pattern detection with combined wavelet subband entropy 4–16 Hz.

The WSE of coefficients (Daubechies 3 mother wavelet) corresponding to a frequency band of 16–32 Hz was found to be the best for spike detection. Spike activity was set to be detected when WSE 16–32 Hz was equal or below the cutoff value 0.80. The ROC curve for spike detection is presented in figure 4.

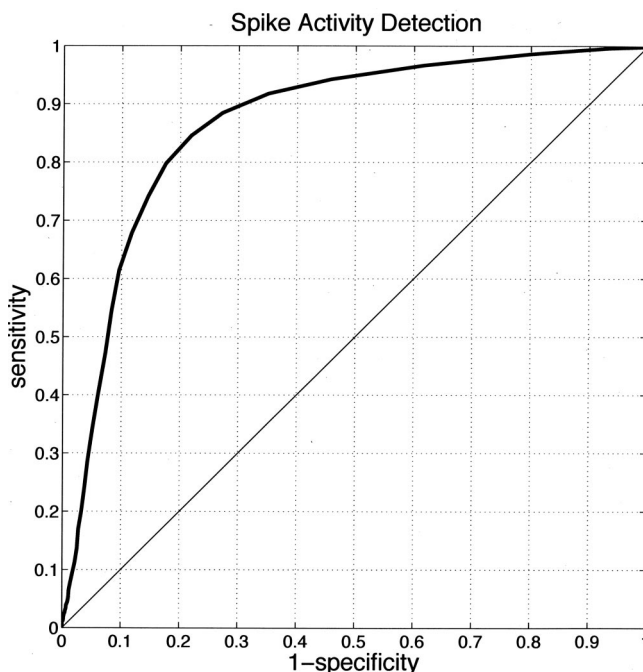


Fig. 4. The receiver operating characteristic curve for spike activity detection with wavelet subband entropy 16–32 Hz.

Performance Evaluation

The P_K value for the cWSE 4–16 Hz ability to follow evolutionary electroencephalographic patterns was 0.809 (SE, 0.007; 95% CI, 0.795–0.823), and for WSE 16–32 Hz the P_K value was 0.804 (SE, 0.007; 95% CI, 0.790–0.818). The P_K value for cWSE 4–16 Hz to detect the presence of monophasic patterns was 0.934 (SE, 0.006; 95% CI, 0.922–0.946), sensitivity 86.1% (SE, 0.4%; 95% CI, 85.3–86.8%), and specificity 87.2% (SE, 0.6%; 95% CI, 86.0–88.4%). The P_K value for WSE 16–32 Hz ability to detect spike activity was 0.868 (SE, 0.008; 95% CI, 0.852–0.884), sensitivity 79.8% (SE, 0.5%; 95% CI, 78.8–80.7%), and specificity 82.5% (SE, 0.6%; 95% CI, 81.4–83.6%).

BIS and WSE during Epileptiform Activity

Using the Kolmogorov-Smirnov test and visual examination of histograms, the distributions of the BIS and WSE values were found to be significantly different from the normal distribution. The medians and quartiles of BIS and both WSE values in each electroencephalographic class are presented in figure 5 and table 3. BIS values decreased with deepening anesthesia from awake to δ ($df = 54$, $P < 0.001$) and from δ to slow δ activity ($df = 40$, $P < 0.001$).

Both WSE variables decreased in a monotonic fashion from class DS to DSM, from DSM to DSMS, and from DSMS to PD. For cWSE 4–16 Hz, class D values are significantly higher than DS ($df = 42$, $P < 0.05$), DS higher than DSM ($df = 39$, $P < 0.001$), DSM higher than DSMS ($df = 24$, $P < 0.001$), and DSMS higher than PD ($df = 21$, $P < 0.05$). For WSE 16–32 Hz, class DS values are significantly higher than DSM ($df = 39$, $P < 0.001$), DSM higher than DSMS ($df = 24$, $P < 0.001$), and DSMS higher than PD ($df = 21$, $P < 0.01$).

The signal quality index and proportion of BIS-not-displayed time for different electroencephalographic classes are presented in table 3. During DSMS and PD activity, the proportion of BIS-not-displayed time tended to increase and SQI tended to decrease. BIS values greater than 60 during the period of deep hypnosis were observed in 34 of the 54 patients. The event sensitivity for detecting this situation was 97.1%. The sensitivity for detection of a BIS reading greater than 60 was 92.5%.

Discussion

We developed a novel feature, wavelet subband entropy, for the monitoring of epileptiform electroencephalographic waveforms occurring in sevoflurane anesthesia. Epileptiform activity during sevoflurane anesthesia is characterized by an evolutionary pattern,^{3,4,6,8,24} starting with gradual slowing of the electroencephalogram (figs. 1A and B), that leads first to appearance of the monophasic pattern (fig. 1C). Later, spike activity starts with a

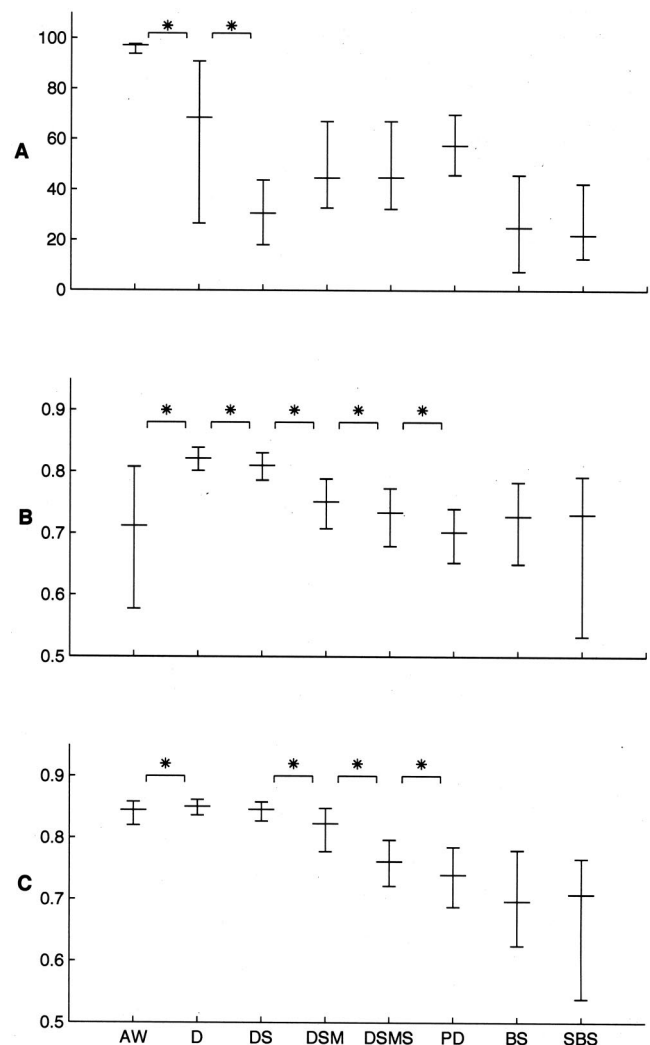


Fig. 5. Median and quartile values of (A) Bispectral Index, (B) combined wavelet subband entropy 4–16 Hz, and (C) wavelet subband entropy 16–32 Hz for each electroencephalographic class. AW = awake activity; BS = burst suppression; D = δ activity; DS = slow δ activity; DSM = slow δ monophasic activity; DSMS = slow δ monophasic activity with spikes; PD = periodic discharges; SBS = burst suppression with spikes. *Statistical significance ($P < 0.05$) between classes.

gradual increase in amplitude and, when evolving further, becomes rhythmic and periodic (figs. 1D–F). The method developed is able to react to the start and end of the epileptiform activity (fig. 6) and to produce consistently decreasing values following the evolutionary pattern described (fig. 5). The method improves understanding of the electroencephalogram-derived information during anesthesia by recognizing and interpreting potentially misleading readings of depth-of-anesthesia monitors. The proposed method provides output that is specific to epileptiform activity and does not react for other electroencephalographic changes occurring during anesthesia.

The method is aimed to be used as a supplementary component for a depth-of-anesthesia monitor, thus improving the reliability of the device. Epileptiform activity

Table 3. BIS, Combined Wavelet Subband Entropy 4–16 Hz, Wavelet Subband Entropy 16–32 Hz, Signal Quality Index of the BIS, and Proportion of BIS-not-displayed Time for Different Electroencephalographic Classes

Class	BIS Median (IQR)	cWSE 4–16 Hz Median (IQR)	WSE 16–32 Hz Median (IQR)	SQI Median (IQR)	Proportion of BIS-not-displayed Time, %
AW	97.2 (93.8–97.6)	0.71 (0.58–0.81)	0.84 (0.82–0.86)	31.7 (20.0–46.7)	12.9
D	68.6 (26.6–90.8)	0.82 (0.80–0.84)	0.85 (0.84–0.86)	66.7 (45.8–96.7)	3.9
DS	30.6 (18.0–43.8)	0.81 (0.79–0.83)	0.85 (0.83–0.86)	90.0 (63.3–96.7)	2.6
DSM	44.7 (32.8–67.0)	0.75 (0.71–0.79)	0.82 (0.78–0.85)	69.2 (43.3–94.2)	5.1
DSMS	44.8 (32.4–67.1)	0.73 (0.68–0.77)	0.76 (0.72–0.80)	66.7 (23.8–90.0)	14.7
PD	57.5 (45.9–69.9)	0.70 (0.65–0.74)	0.74 (0.69–0.78)	65.8 (38.3–86.7)	10.0
BS	25.0 (7.6–45.9)	0.73 (0.65–0.78)	0.70 (0.62–0.78)	96.7 (81.7–100.0)	1.6
SBS	22.0 (12.8–42.5)	0.73 (0.53–0.79)	0.71 (0.54–0.77)	81.7 (59.8–95.8)	0.6

AW = awake activity; BIS = Bispectral Index; BS = burst suppression; cWSE = combined wavelet subband entropy; D = δ activity; DS = slow δ activity; DSM = slow δ monophasic activity; DSMS = slow δ monophasic activity with spikes; IQR = interquartile range; PD = periodic discharges; SBS = burst suppression with spikes; SQI = signal quality index; WSE = wavelet subband entropy.

during sevoflurane mask induction, although generalized, has been shown to be predominant in the frontal region,⁸ therefore making depth-of-anesthesia monitors especially vulnerable to these waveforms. With sevoflurane, epileptiform activity in neurologically healthy subjects is typically observed in deep anesthesia,^{8,24} although patients with brain lesions, even without symptoms, may exhibit seizure activity also during the emergence phase.²⁵

The developed method identifies otherwise unexplained increases or fluctuations of the monitor, thereby assisting to optimize anesthetic drug administration. Targeting BIS to 40–60 during the maintenance phase decreases the use of sevoflurane by 29% compared with the control group.²⁶ Our data demonstrate BIS values greater than 60 in 63% of patients during deep level of sevoflurane-induced hypnosis with epileptiform activity. The proposed method detected this with event sensitivity of 97.1%. Only a single BIS reading of 62 in a patient whose electroencephalogram otherwise had BIS values less than 60 remained undetected. Further, we illustrated that BIS tends to display no index value on the monitor screen during epileptiform electroencephalographic activity. The high proportion of BIS-not-displayed time during DSMS and PD activity may be caused by the BIS algorithm assuming these waveforms to be artifacts. The distribution of SQI values supports this assumption. In our visual analysis from these time periods, we did not observe a large number of artifacts.

In a previous study,⁶ we showed that patients with rhythmic or periodic spike activity experienced a simultaneous increase in heart rate, and patients without such activity did not show the increase. Involvement of the cardiovascular system in ongoing epileptiform activity may imply a more severe type of electroencephalographic abnormality. This has been demonstrated especially in electroconvulsive therapy, where seizures are associated with a hemodynamic arousal.^{27,28} Several studies have shown an increase of heart rate during seizures.^{29–32} Periodic discharges have been hypothe-

sized to represent the last of the progressive electroencephalographic stages of untreated generalized convulsive status epilepticus.³³ That stage is accompanied with the reduction in the cerebral blood flow and brain glucose level, a further decline in brain oxygenation, thus creating a risk for an irreversible brain damage.³⁴ In sevoflurane anesthesia, periodic discharges have been demonstrated to precede the seizure.^{3,24} These aspects support our hypothesis of the adverse nature of periodic discharges. As demonstrated by a P_K value of 0.8 and figure 5, WSE consistently decreased with an increasing severity of epileptiform activity. Further studies are needed to estimate ability of our method to predict seizures in sevoflurane anesthesia.

The advantage of having two variables, sensitive to electroencephalographic changes in different frequency bands, becomes clear when one observes the distribution of WSE values over different electroencephalographic classes. The most prominent decrease in median values for cWSE 4–16 Hz was between classes DS and DSM, and with WSE 16–32 Hz it was between classes DSM and DSMS (fig. 5). cWSE 4–16 Hz proved to be useful as a predictive indicator of spike activity. Visual classification of the electroencephalogram with 1-s resolution was a demanding task because electroencephalographic activity continuously evolved and, although most patterns were recognizable, discrimination between some classes was difficult. Given these difficulties, the P_K values for the evolutionary patterns are encouraging. Performance measures for detection of the monophasic pattern were better than those for spike detection. This was probably partly due to high-frequency noise corrupting some recordings, complicating the recognition of spikes.

Spike activity was easily captured by one frequency band only. For the monophasic pattern monitoring, we used the combination of two adjacent frequency bands, because that improved sensitivity during the emerging phase of monophasic pattern (fig. 7). Additional analysis with DS and DSM classes only was reasonable, because the initial analysis contained a substantial amount data

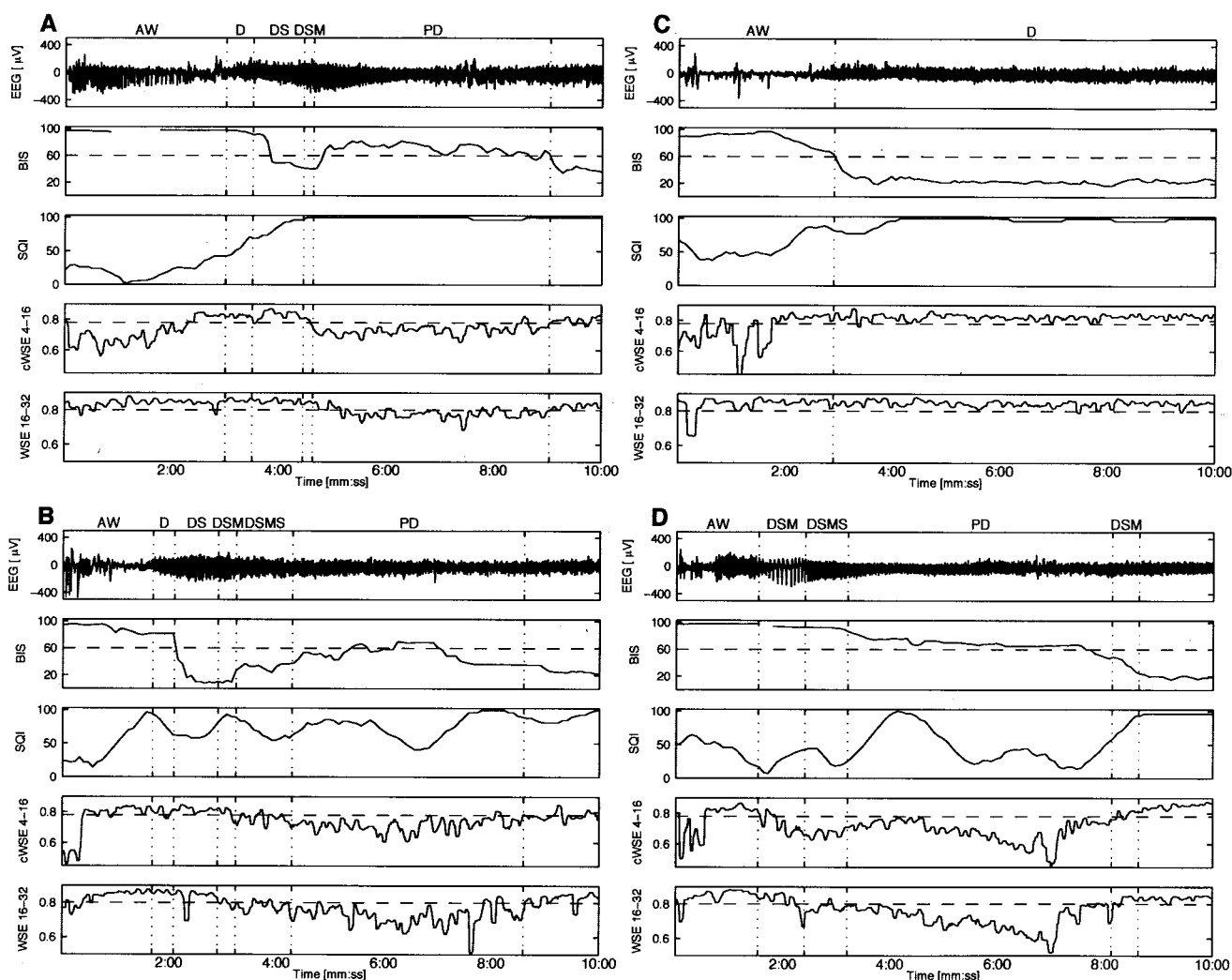


Fig. 6. Examples of the behavior of electroencephalogram (EEG), Bispectral Index (BIS), signal quality index (SQI), combined wavelet subband entropy (cWSE) 4–16 Hz, and wavelet subband entropy (WSE) 16–32 Hz during four sevoflurane inductions; each graph contains 10 min of the recordings. Horizontal dashed lines correspond to a BIS level of 60 and cutoff values for cWSE 4–16 Hz and WSE 16–32 Hz, which are 0.78 and 0.80, respectively. Vertical dotted lines correspond to the boundaries of visual electroencephalogram classification. AW = awake activity; D = δ activity; DS = slow δ activity; DSM = slow δ monophasic activity; DSMS = slow δ monophasic activity with spikes; PD = periodic discharges. (A) BIS decreased below 60 during DS and DSM activity. At the onset of PD activity, BIS increased to greater than 60 and remained there until the end of PD activity. The SQI remained high during the epileptiform activity. Both WSE variables reacted to the onset and end of PD activity. (B) BIS decreased below 20, indicating deep anesthesia. When the DSMS pattern appeared in the electroencephalogram, BIS began a gradual increase, exceeding 60 during PD activity. After the end of PD activity, BIS returned to a level indicating deep anesthesia. WSE variables gradually decreased during epileptiform electroencephalographic periods and returned to their baseline levels when PD activity disappeared. (C) For the patient without epileptiform activity, BIS worked reliably, and during anesthesia, WSE variables remained above their cutoff values. (D) BIS remained high when the AW pattern immediately turned into DSM activity. A decrease in the cWSE 4–16 Hz variable indicated the appearance of the monophasic pattern; later, spikes appeared in the electroencephalogram, resulting in a gradual decrease for WSE 16–32 Hz.

from the PD class (table 1), which is not necessarily characterized by the monophasic pattern (fig. 1: compare C and D with E and F). As expected, the monophasic pattern was best detected with Daubechies 1 (also known as the Haar wavelet), which can be represented with the step function and thought of as a sequence of square waves. Spikes were best detected with Daubechies 3, which has similarities with the morphology of epileptiform spikes (fig. 2).

During burst suppression, variability in both WSE variables was high. Suppressions longer than or equal to 5 s

result in high WSE values, because the signal of the analyzed epoch is flat and entropy of a flat distribution is high. However, during burst suppression, the BIS value is highly influenced by the BSR. It has been shown with an A-1000[®] monitor that BIS can be estimated with the equation $BIS = 50 - BSR/2$, when the BSR is greater than 40%.³⁵ With the newer A-2000[®] monitor, a relation between BIS and BSR is still present, although the equation is slightly different.^{13,36} The BIS algorithm's burst suppression detection seemed reliable also during epileptiform burst suppression periods, resulting in reason-

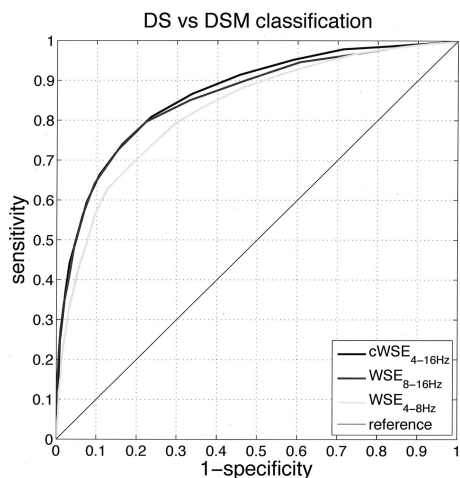


Fig. 7. The receiver operating characteristic curve for the monophasic pattern detection with combined wavelet subband entropy (cWSE) 4–16 Hz, wavelet subband entropy (WSE) 8–16 Hz, and WSE 4–8 Hz when only slow δ activity (DS) and slow δ monophasic activity (DSM) classes are used in the analysis. Generally, cWSE 4–16 Hz had a better sensitivity than WSE 8–16 Hz at the important stage when a monophasic pattern emerged and was selected for the final implementation.

able BIS values. Therefore, we concentrated on the data before burst suppression.

In the study by Jääskeläinen *et al.*,²⁴ epileptiform activity occurred in all eight subjects at the burst suppression level of steady state sevoflurane anesthesia. Previously, Kaisti *et al.*⁵ had used the same data set and reported BIS values of 44 and 73 with two subjects having epileptiform discharges. The probable reason for high BIS values in only two subjects was that all patients were at burst suppression level and BIS was influenced by the BSR. This may be the explanation also for the results of Julliac *et al.*,⁸ where a BIS increase greater than 20 was observed in 5 of the 11 patients with epileptiform activity. In our data set, epileptiform activity preceded burst suppression, thus being the probable reason for the higher incidence of the high BIS values. This may be related to the activating effects of nitrous oxide to the burst suppression electroencephalogram.³⁷ Otherwise, data obtained in other studies^{8,24} contained similar electroencephalographic patterns, occurring in the same sequence as in our data. Similar patterns have occurred also with sevoflurane mask-induced anesthesia in children.⁷ Several new versions of the BIS algorithm have been released since version 3.0. However, we are not aware of any improvements in the algorithm regarding epileptiform activity. A recent study of Julliac *et al.*⁸ with an A-2000[®] monitor (XP platform) demonstrated that the problem still exists. The current recommendation of Aspect Medical Systems is to look at the raw electroencephalographic waveform when epileptiform activity is suspected.³⁸

We will continue development of the algorithm for the burst suppression level. Once the method is fine-tuned to work reliably during burst suppression, WSE variables

can be monitored throughout the whole range of the anesthesia electroencephalogram. Also, the method may prove useful in the monitoring of status epilepticus patients, whose electroencephalographic waveforms exhibit similarities to the epileptiform electroencephalogram in sevoflurane anesthesia.^{33,39}

Eye movements caused low values of cWSE 4–16 Hz during the awake state. Thus far, we have tested our method only with the epileptiform electroencephalogram in sevoflurane anesthesia, and in these circumstances, epileptiform activity is not suspected with awake patients moving their eyes. To further improve the reliability of the method, eye movement artifacts can be detected with the separate technique using, for example, template matching, and WSE calculation can be eliminated in the case of detected eye movements. Also, cardiac artifacts may influence WSE variables; simultaneous electrocardiogram measurement is required for eliminating this effect.

Besides improving the reliability of electroencephalographic monitoring during sevoflurane anesthesia, the developed method may have benefits to avoid epileptiform electroencephalographic and seizure activity during any kind of anesthesia. Seizures during anesthesia, although not common, are likely to increase costs. Patients may become admitted to the intensive care unit or they may have a prolonged follow-up with subsequent detailed neurologic testing^{24,40} and brain scans.^{24,25}

In the past, patients were reassured that there were risks for damage only when seizures were prolonged, as in status epilepticus. Emerging experimental studies in chronic models, human magnetic resonance imaging, and neuropsychological studies have provided new information about adverse long-term consequences of seizures. There is increasing evidence that single seizures and repeated brief seizures evoked by kindling produce neuronal damage and brain cell death. A single kindled seizure doubles the rate of apoptosis in the hilar neurons of the dentate gyrus.⁴¹ Seizure-induced cell death and damage may adversely affect functional properties of neural circuits and networks, and subtle seizure-induced neuronal loss or circuit reorganization could have clinically significant impact on cognition and behavior.⁴¹ Although seizure-induced damage seems less prominent in the immature nervous system, early life seizures have adverse effects on a variety of cognitive and behavioral domains.⁴¹ These observations should be carefully taken into account when administering sevoflurane, especially because of its popularity in pediatrics. We did not record seizure activity, and our patients had an uneventful postanesthetic recovery.

Currently available electroencephalographic monitors for anesthesia practice do not offer automatic recognition of epileptiform activity. Therefore, the incidence of epileptiform electroencephalogram in sevoflurane anesthesia is not known and may be more common than

expected. Several reports of seizure-like phenomena with patients in propofol anesthesia also exist, but few of these have accompanying electroencephalographic recordings.⁴⁰ Clinical detection of intraoperative seizures are difficult because neuromuscular blocking agents are commonly used.

Wavelet subband entropy variables proved successful in detecting and quantifying sevoflurane-induced epileptiform activity and are suggested as a promising method for the prediction and prevention of epileptiform activity during sevoflurane anesthesia.

References

1. Sarner JB, Levine M, Davis PJ, Lerman J, Cook DR, Motoyama EK: Clinical characteristics of sevoflurane in children: A comparison with halothane. *ANESTHESIOLOGY* 1995; 82:38-46
2. Thwaites A, Edmonds S, Smith I: Inhalation induction with sevoflurane: A double-blind comparison with propofol. *Br J Anaesth* 1997; 78:356-61
3. Woodforth IJ, Hicks RG, Crawford MR, Stephen JPH, Burke DJ: Electroencephalographic evidence of seizure activity under deep sevoflurane anesthesia in a nonepileptic patient. *ANESTHESIOLOGY* 1997; 87:1579-82
4. Yli-Hankala A, Vakkuri A, Särkelä M, Lindgren L, Korttila K, Jääntti V: Epileptiform electroencephalogram during mask induction of anesthesia with sevoflurane. *ANESTHESIOLOGY* 1999; 91:1596-603
5. Kaisti KK, Jääskeläinen SK, Rinne JO, Metsähonkala L, Scheinin H: Epileptiform discharges during 2 MAC sevoflurane anesthesia in two healthy volunteers. *ANESTHESIOLOGY* 1999; 91:1952-5
6. Vakkuri A, Jääntti V, Särkelä M, Lindgren L, Korttila K, Yli-Hankala A: Epileptiform EEG during sevoflurane mask induction: Effect of delaying the onset of hyperventilation. *Acta Anaesthesiol Scand* 2000; 44:713-9
7. Vakkuri A, Yli-Hankala A, Särkelä M, Lindgren L, Mennander S, Korttila K, Saarnivaara L, Jääntti V: Sevoflurane mask induction of anaesthesia is associated with epileptiform EEG in children. *Acta Anaesthesiol Scand* 2001; 45:805-11
8. Julliac B, Guehl D, Chopin F, Arne P, Burbaud P, Sztark F, Cros A-M: Risk factors for the occurrence of electroencephalogram abnormalities during induction of anesthesia with sevoflurane in nonepileptic patients. *ANESTHESIOLOGY* 2007; 106:243-51
9. Adachi M, Ikemoto Y, Kubo K, Takuma C: Seizure-like movement during induction of anaesthesia with sevoflurane. *Br J Anaesth* 1992; 68:214-5
10. Rampil IJ: A primer for EEG signal processing in anesthesia. *ANESTHESIOLOGY* 1998; 89:980-1002
11. Katoh T, Suzuki A, Ikeda K: Electroencephalographic derivatives as a tool for predicting the depth of sedation and anesthesia induced by sevoflurane. *ANESTHESIOLOGY* 1998; 88:642-50
12. Olofsen E, Dahan A: The dynamic relationship between end-tidal sevoflurane and isoflurane concentrations and Bispectral Index and spectral edge frequency of the electroencephalogram. *ANESTHESIOLOGY* 1999; 90:1345-53
13. Ellerkmann RK, Liermann V-M, Alves TM, Wenningmann I, Kreuer S, Wilhelm W, Roepcke H, Hoefl A, Bruhn J: Spectral entropy and Bispectral Index as measures of the electroencephalographic effects of sevoflurane. *ANESTHESIOLOGY* 2004; 101:1275-82
14. Chinzei M, Sawamura S, Hayashida M, Kitamura T, Tamai H, Hanaoka K: Change in Bispectral Index during epileptiform electrical activity under sevoflurane anesthesia in a patient with epilepsy. *Anesth Analg* 2004; 98:1734-6
15. Mallat SG: A theory for multiresolution signal decomposition: The wavelet representation. *IEEE Trans Pattern Anal Mach Intell* 1989; 11:674-93
16. Smith NJ, van Gils M, Prior P: Neurophysiological Monitoring during Intensive Care and Surgery. Amsterdam, The Netherlands, Elsevier, 2006, pp 11, 340-4
17. Coifmann RR, Wickerhauser MV: Entropy-based algorithms for best basis selection. *IEEE Trans Inf Theory* 1992; 38:713-8
18. Daubechies I: Ten Lectures on Wavelets, 9th printing Philadelphia, Society for Industrial and Applied Mathematics, 2006, pp 15, 197
19. Misioti M, Misioti Y, Oppenheim G, Poggi J-M: Wavelet Toolbox User's Guide. Natick, MA, The MathWorks, 1997-2007
20. Shannon CE, Weaver W: The Mathematical Theory of Communication. Urbana and Chicago, University of Illinois Press, 1998, pp 48-56
21. Pudil P, Novovičová J, Kittler J: Floating search methods in feature selection. *Patt Rec Lett* 1994; 15:1119-25
22. Smith WD, Dutton RC, Smith NT: Measuring the performance of anesthetic depth indicators. *ANESTHESIOLOGY* 1996; 84:38-51
23. Wilson SB: Algorithm architectures for patient dependent seizure detection. *Clin Neurophysiol* 2006; 117:1204-16
24. Jääskeläinen K, Kaisti K, Suni L, Hinkka S, Scheinin H: Sevoflurane is epileptogenic in healthy subjects at surgical levels of anesthesia. *Neurology* 2003; 61:1073-8
25. Hilty CA, Drummond JC: Seizure-like activity on emergence from sevoflurane anesthesia. *ANESTHESIOLOGY* 2000; 93:1357-9
26. Aimé I, Verroust N, Masson-Lefoll C, Taylor G, Laloë P-A, Liu N, Fischler M: Does monitoring Bispectral Index or spectral entropy reduce sevoflurane use? *Anesth Analg* 2006; 103:1469-77
27. Castelli I, Steiner LA, Kaufmann MA, Alfille PH, Schouten R, Welch CA, Drop IJ: Comparative effects of esmolol and labetalol to attenuate hyperdynamic states after electroconvulsive therapy. *Anesth Analg* 1995; 80:557-61
28. Fu W, Stool LA, White PF, Husain MM: Is oral clonidine effective in modifying the acute hemodynamic response during electroconvulsive therapy? *Anesth Analg* 1998; 86:1127-30
29. Blumhardt LD, Smith PE, Owen L: Electrocardiographic accompaniments of temporal lobe epileptic seizures. *Lancet* 1986; 8489:1051-6
30. Keilson MJ, Hauser WA, Magrill JP: Electrocardiographic changes during electrographic seizures. *Arch Neurol* 1989; 46:1169-70
31. Nousiainen U, Mervaala E, Ylinen A, Uusitupa M, Riekkinen P: The importance of electrocardiogram in ambulatory electroencephalographic recordings. *Arch Neurol* 1989; 46:1171-4
32. Zijlmans M, Flanagan D, Gotman J: Heart rate changes and ECG abnormalities during epileptic seizures: Prevalence and definition of an objective clinical sign. *Epilepsia* 2002; 43:847-54
33. Treiman DM, Walton NY, Kendrick C: A progressive sequence of electroencephalographic changes during generalized convulsive status epilepticus. *Epilepsy Res* 1990; 5:49-60
34. Young GB: Status epilepticus and brain damage: Pathology and pathophysiology. *Advances in Neurology*, Vol. 97: Intractable Epilepsies. Edited by Blume WT, Carlen PL, Starreveld E, Wiebe S, Young GB. Philadelphia, Lippincott Williams & Wilkins, 2006, pp 217-20
35. Bruhn J, Bouillon TW, Shafer SL: Bispectral index (BIS) and burst suppression: Revealing a part of the BIS algorithm. *J Clin Monit Comput* 2000; 16:593-6
36. Vakkuri A, Yli-Hankala A, Talja P, Mustola S, Tolvanen-Laakso H, Sampson T, Viertiö-Oja H: Time-frequency balanced spectral entropy as a measure of anesthetic drug effect in central nervous system during sevoflurane, propofol, and thiopental anesthesia. *Acta Anaesthesiol Scand* 2004; 48:145-53
37. Yli-Hankala A, Lindgren L, Porkkala T, Jääntti V: Nitrous oxide-mediated activation of the EEG during isoflurane anaesthesia in patients. *Br J Anaesth* 1993; 70:54-7
38. Kelley SD: Monitoring Level of Consciousness during Anesthesia and Sedation: A Clinician's Guide to the Bispectral Index®. Norwood, MA, Aspect Medical Systems, 2003, p 6-5
39. Treiman DM: Electroclinical features of status epilepticus. *J Clin Neurophysiol* 1995; 12:343-62
40. Walder B, Tramèr MR, Seck M: Seizure-like phenomena and propofol: A systematic review. *Neurology* 2002; 58:1327-32
41. Sutula TP, Hagen J, Pitkänen A: Do epileptic seizures damage the brain? *Curr Opin Neurol* 2003; 16:189-95